J. Synchrotron Rad. (1998). **5**, 1013–1015

Spectrometer for polarized soft X-ray Raman scattering

Y. Harada,[a]* H. Ishii,[a] M. Fujisawa,[a] Y. Tezuka,[a] S. Shin,[a] M. Watanabe,[b] Y. Kitajima[b] and A. Yagishita[b]

[a]*Synchrotron Radiation Laboratory, Institute for Solid State Physics, University of Tokyo, Tanashi, Tokyo 188, Japan, and* [b]*Photon Factory, Institute of Materials Structure Science, Tsukuba, Ibaraki 305, Japan.*
E-mail: harada@issp.u-tokyo.ac.jp

(*Received 4 August 1997; accepted 15 December 1997*)

An experimental system for polarized soft X-ray Raman scattering spectroscopy has been constructed. The soft X-ray spectrometer is based on the Rowland circle geometry with a holographic spherical grating. Three types of gratings are used to cover the energy range from 18 eV to 1200 eV. According to a ray-trace simulation, the resolution is expected to be 200 meV at 700 eV by using a 10 μm slit width. The polarized and depolarized soft X-ray Raman scattering spectra can be measured by rotating the soft X-ray spectrometer around the axis of the incident beam. Preliminary measurements of polarized and depolarized spectra were accomplished at undulator beamline BL-2C of the Photon Factory.

Keywords: soft X-ray emission; fluorescence; Raman scattering; Rowland circles; spherical gratings.

1. Introduction

Soft X-ray emission spectroscopy (SXES) has provided us with fruitful information about the electronic structure of matter (Callcott *et al.*, 1986; Nordgren *et al.*, 1989; Ma *et al.*, 1992; Shin *et al.*, 1995; Ederer & McGuire, 1996). SXES reflects the local partial density of states depending on the produced core hole. Furthermore, it is well known that the emission spectra consist of not only the fluorescence component but also the inelastic scattering component called Raman scattering. When the electron is excited to the conduction band by soft X-ray light, an emission is caused from the valence band, so that a pair of the conduction electron and the valence hole remains as an elementary excitation of Raman scattering. Raman scattering is the two-photon process as a coherent optical process so that it is thought that the polarization dependence of the incident and emission lights gives fruitful information on the electronic structure (Guo *et al.*, 1995).

In this paper, we report the construction of a spectrometer for polarized soft X-ray Raman scattering in order to measure the polarization dependence of soft X-ray Raman scattering. It has been installed on the undulator beamline BL-2C at the Photon Factory (Watanabe *et al.*, 1997) and preliminary polarization dependence was measured on CaO.

2. Experiment

The system consists of an analyser chamber and a sample-preparation chamber. The analyser chamber is equipped with a soft X-ray emission spectrometer and a commercially available photoelectron spectrometer (VG-CLAM2), which enables us to calibrate the incident photon energy, and a SXES spectrometer. Samples can be cooled to 15 K using a manipulator with an He refrigerator.

Fig. 1 shows a front view of the system. The analyser chamber can be rotated by 90° together with the spectrometer and the photoelectron analyser around the axis of the incident photon beam; the rotation centre is located at the sample position. The analyser chamber is sealed with two differentially pumped rotary feed-throughs, and is connected to the sample-preparation chamber. The sample-preparation chamber has a small air-lock chamber for inserting many samples from the atmosphere.

In beamline BL-2C, the electric field of the incident photon is polarized in the horizontal plane. When the SXES is measured by the 'depolarized' configuration, as shown in Fig. 1(*a*), the polarization of SXES rotates by 90° from the polarization of the incident light. On the other hand, when the SXES is measured by the 'polarized' configuration, as shown in Fig. 1(*b*), the polarization of SXES contains the same polarization as the incident light.

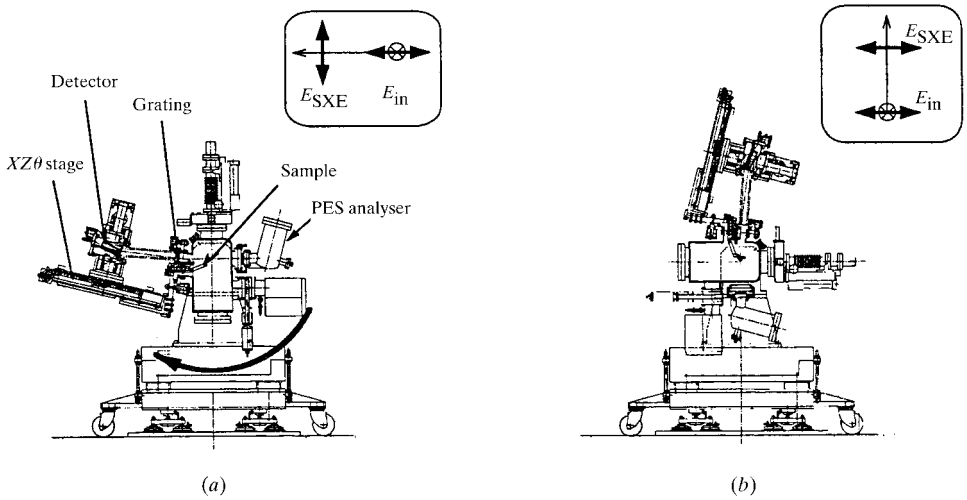

Figure 1
Side view of the spectrometer. (*a*) In the depolarized configuration the electric fields of SXES rotate from that of the incident light, while in (*b*) the polarized configuration has the same polarization as that of the incident light. The insets show the polarizations of the incident photon (E_{in}) and that of the SXES (E_{SXE}).

The spectrometer uses the Rowland circle geometry, in which an incidence slit, gratings and a detector are located. The focal planes of the spectrometer for three gratings are shown in Fig. 2. The slit is located 10 mm from the sample. Available slit widths are 10, 20, 50, 100 and 300 μm. The lengths between the slit and the gratings are the same for each grating. The detector is numerically positioned tangentially on the Rowland circle by the three-axis control of two translations and one rotation using pulse motors. Three laminar-type holographic spherical gratings have been prepared to cover the photon energy range from 18 to 1200 eV. We can choose two gratings in a spectrometer at one time according to the desired energy range. Two gratings are changeable in the vacuum.

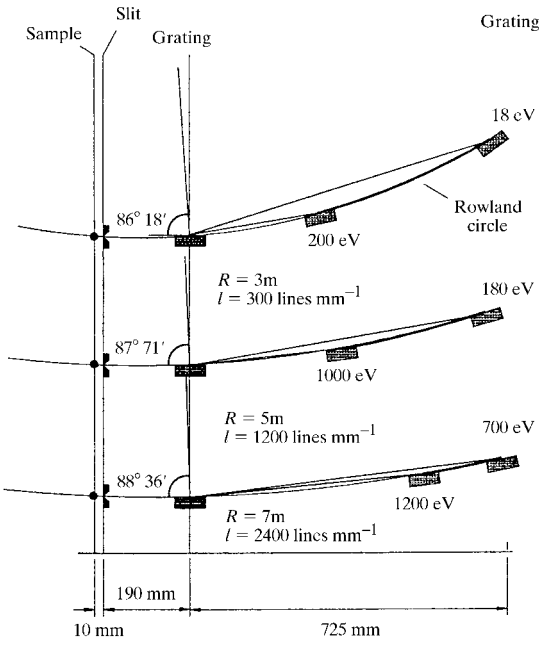

Figure 2
Focal planes of the spectrometer for three gratings.

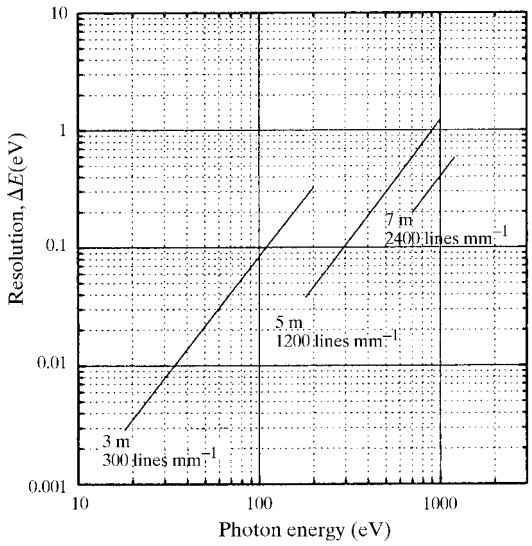

Figure 3
Energy resolution ΔE for three gratings obtained by the ray tracing with 10 μm slit width. The curves are labelled with ruling density (lines mm^{-1}) and grating radii (m).

In order to compensate the distortion of the slit image, a multichannel detector is used. To increase the quantum efficiency of the detector we adopt a wire in front of the microchannel plate, whose surface is coated with CsI.

3. Results and discussion

Fig. 3 shows the energy resolution calculated by the ray tracing when the 10 μm slit width is used. The spot size on the sample is 8 μm × 100 μm at BL-2C. An energy resolution of 200 meV can be reached at 700 eV by using a 7 m-radius grating, and 40 meV can be reached at 200 eV by using a 5 m-radius grating.

Several transition-metal compounds and rare-earth compounds have been measured by using this system. The preliminary measurement on CaO for the polarization dependence of SXES is shown in Fig. 4. Fig. 4(*a*) shows the Ca 2*p* total photon yield (TPY) spectrum of CaO. The numbers on the spectrum indicate the excitation energies of Ca 2*p* SXES spectra. Solid and dotted lines in Fig. 4(*b*) show the Ca 2*p* SXES spectra measured by depolarized and polarized configurations, where the spectra were smoothed. The abscissa is the shift energy from the incident photon energy. The spectra have three structures at 9.0, 11.5 and 13.0 eV. When t_{2g} symmetric point (No. 2) is excited, a structure around 13.0 eV is dominant. When e_g symmetric points (No. 3,

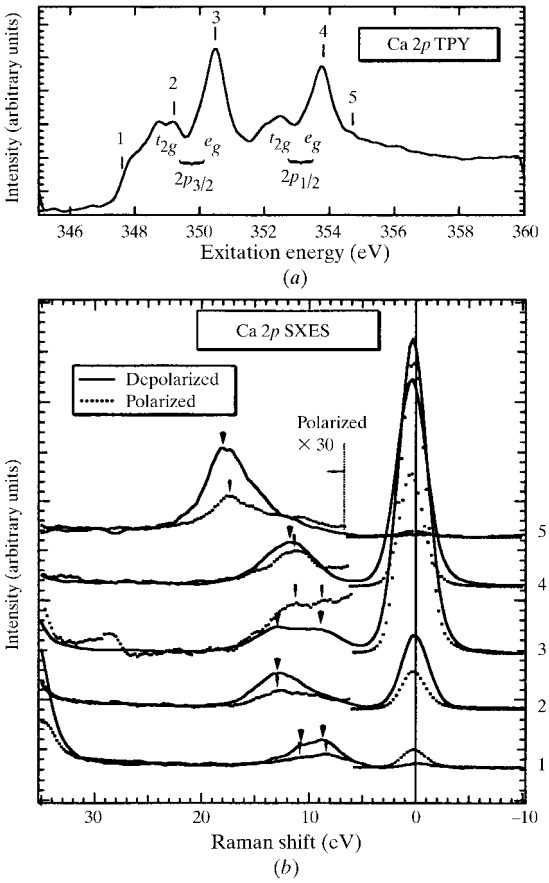

Figure 4
(*a*) Ca 2*p* total yield spectrum of CaO. The vertical bars on the spectrum indicate the excitation energies of measured Ca 2*p* SXES spectra. (*b*) Smoothed Ca 2*p* SXES spectra. The abscissa is the loss energy from the excitation photon energy. The solid line shows the depolarized configuration and the dotted line shows the polarized configuration.

No. 4) are excited, a structure around 11.5 eV appears. These inelastic peaks are well elucidated by the calculated band dispersion curve of CaO.

The No. 3 spectra have a rather strong polarization dependence, *i.e.* the polarized spectrum has a structure at 11.5 eV, while the depolarized spectrum has a structure at 13.0 eV. There are two structures for L valence bands, *i.e.* L_5 and L_1. The structure at 11.5 eV may correspond to the energy separations between the valence L_5 and conduction L_5 states, while the structure at 13.0 eV may correspond to the energy separation between L_1 and L_5 states.

CaO has an NaCl-type cubic crystal structure. Even in the cubic crystal the polarization of the SXES would show fruitful results for the electronic structure of matter.

References

Callcott, T. A., Tsang, K. L., Zhang, C. H., Ederer, D. L. & Arakawa, E. T. (1986). *Rev. Sci. Instrum.* **57**, 2680–2690.

Ederer, D. L. & McGuire, J. H. (1996). Editors. *Raman Emission by X-ray Scattering.* Singapore: World Scientific.

Guo, J.-H., Wassdahl, N., Skytt, P., Butorin, S. M., Duda, L.-C., Englund, C. J. & Nordgren, J. (1995). *Rev. Sci. Instrum.* **66**, 1561–1563.

Ma, Y., Wassdahl, N., Skytt, P., Guo, J.-H., Nordgren, J., Johnson, P. D., Rubensson, J.-E., Boske, T., Eberhardt, W. & Kevan, S. D. (1992). *Phys. Rev. Lett.* **69**, 2598–2601.

Nordgren, J., Bray, G., Cramm, S., Nyholm, R., Rubensson, J.-E. & Wassdahl, N. (1989). *Rev. Sci. Instrum.* **60**, 1690–1696.

Shin, S., Agui, A., Fujisawa, M., Tezuka, Y. & Ishii, T. (1995). *Rev. Sci. Instrum.* **66**, 1584–1586.

Watanabe, M., Toyoshima, A., Azuma, Y., Hayaishi, T., Yan, Y. & Yagishita, A. (1997). *SPIE*, **3150**, 58–66.